

Singlet–Triplet Energy Splitting and Excited States of Phenylnitrene

Michael Winkler*

Institut für Organische Chemie, Universität Würzburg, Am Hubland, 97074 Würzburg, Germany

Received: March 24, 2008; Revised Manuscript Received: May 19, 2008

The vertical and adiabatic singlet–triplet energy splittings (ΔE_{ST}) of phenylnitrene were computed by a variety of multireference configuration interaction and perturbation theory methods employing basis sets of up to quadruple- ξ quality and extrapolation to the complete basis set limit. The vertical and adiabatic energy gaps are 18.9 and 15.9 kcal mol⁻¹, respectively, the latter in reasonable agreement with the revised experimental value of 15.1 \pm 0.2 kcal mol⁻¹. The energy difference between both states at the geometry of the \tilde{a}^1A_2 singlet state was also considered and amounts to 13.8 kcal mol⁻¹. In obtaining accurate state energy splittings, basis set completeness turns out to be a more important issue than the level of dynamical electron correlation treatment. Density functional theory that is frequently employed to investigate phenylnitrenes and their rearrangements yields varying results and, depending on the functional, gives adiabatic energy differences between 9 and 16 kcal mol⁻¹. The \tilde{b}^1A_1 state has a similar geometry as the ground state of **1** and is 31 kcal mol⁻¹ higher in energy. According to best estimates, the next higher singlet states, \tilde{c}^1A_1 and \tilde{d}^1B_1 , are 57 and 72 kcal mol⁻¹ above the ground state. In the triplet manifold, vertical excitation energies to the \tilde{A}^3B_1 and \tilde{B}^3A_2 states are 71 and 77 kcal mol⁻¹, respectively.

Introduction

Phenylnitrenes are among the most thoroughly investigated reactive intermediates that are readily available from the photolysis or thermolysis of aryl azides.¹ The reactivity of these intermediates strongly depends on the conditions under which they are formed and the electronic state from which further reactions take place. It is well-established experimentally^{1,2} as well as computationally^{1,3} that the parent phenylnitrene (**1**) has a \tilde{X}^3A_2 triplet ground state in which the formally nonbonding orbitals 8b₂ and 3b₁ are singly occupied (Figure 1). The first excited singlet state (\tilde{a}^1A_2) has the same open-shell electronic configuration. The next higher-lying excited states \tilde{b}^1A_1 and \tilde{c}^1A_1 are closed-shell singlets with a significant two-configurational character and leading configurations (8b₂)² and (3b₁)², respectively.³ Intermolecular rearrangements of **1** at temperatures above 165 K frequently take place from the \tilde{a}^1A_2 state that is initially generated from azide precursors, whereas at lower temperatures, intersystem crossing to the triplet ground state is usually preferred.^{3g}

The adiabatic excitation energies to the first two singlet states were determined by negative ion photoelectron spectroscopy to be 18.3 \pm 0.7 and 30 \pm 5 kcal mol⁻¹, respectively.^{2b,c} The former value was reconsidered recently, and an improved ΔE_{ST} of 15.1 \pm 0.2 kcal mol⁻¹ was reported.⁴ Computationally, the lowest electronic states of **1** were subject to various studies.³ Early work up to 2000 was summarized in a recent review by Karney and Borden.³ⁱ At the highest level of theory published so far, Gritsan and co-workers investigated the vertical excitation energies of singlet and triplet phenylnitrene at the CASPT2 level.^{3g} In our recent work on dehydrophenylnitrenes and didehydrophenylnitrenes, we found it useful to refer to the ground- and excited-state properties and energies of **1** to rationalize the more complex electronic structures of these derivatives.⁵ As part of these studies, we present in this paper a detailed investigation of

the excited states of phenylnitrene employing highly accurate multireference configuration interaction methods and a systematic investigation of basis set convergence with a special focus on the singlet–triplet gap of **1**.

Theoretical Methods and Computational Details

Geometries of the \tilde{X}^3A_2 , \tilde{a}^1A_2 , and \tilde{b}^1A_1 states of **1** were optimized at the complete active space self-consistent field (CASSCF) level;⁶ the (8,8) active space covers the six benzene valence π orbitals and the two formally singly occupied p orbitals at nitrogen (Figure 1). This wave function also served as reference in all multireference (MR) calculations discussed in this work. Dynamical electron correlation was accounted for by Rayleigh–Schrödinger perturbation theory to second (RS2) or third order (RS3)⁷ or by truncated configuration interactions including single and double excitations (CISD) from the reference configurations.⁸ Internal contraction was applied throughout to keep the number of configurations in the CI expansion manageable, whereas only the doubly external excitations were contracted in perturbation theory. Because of the lack of size-extensivity of truncated CI wave functions, the latter approach requires additional corrections (e.g., the Davidson correction, denoted as CISD + Q).⁹ Alternatively, corrections inspired by the cluster expansion were applied, as in the multireference averaged quadratic coupled-cluster (AQCC) and multireference averaged coupled-pair functional (ACPF) methods.¹⁰ The latter is generally considered to represent a particularly suitable compromise between multireference and size-extensivity effects. If not mentioned otherwise, energies of higher excited states within a given irreducible representation are derived from state-specific calculations, but generally, state-averaged computations were carried out for comparison. The frozen-core approximation was applied in all ab initio calculations. Apart from these high-level approaches, the lowest electronic singlet and triplet states also were optimized by various unrestricted DFT methods. The cc-pVXZ family of Dunning's polarized correlation-consistent basis sets (employing

* Corresponding author. E-mail: winkler@chemie.uni-wuerzburg.de.

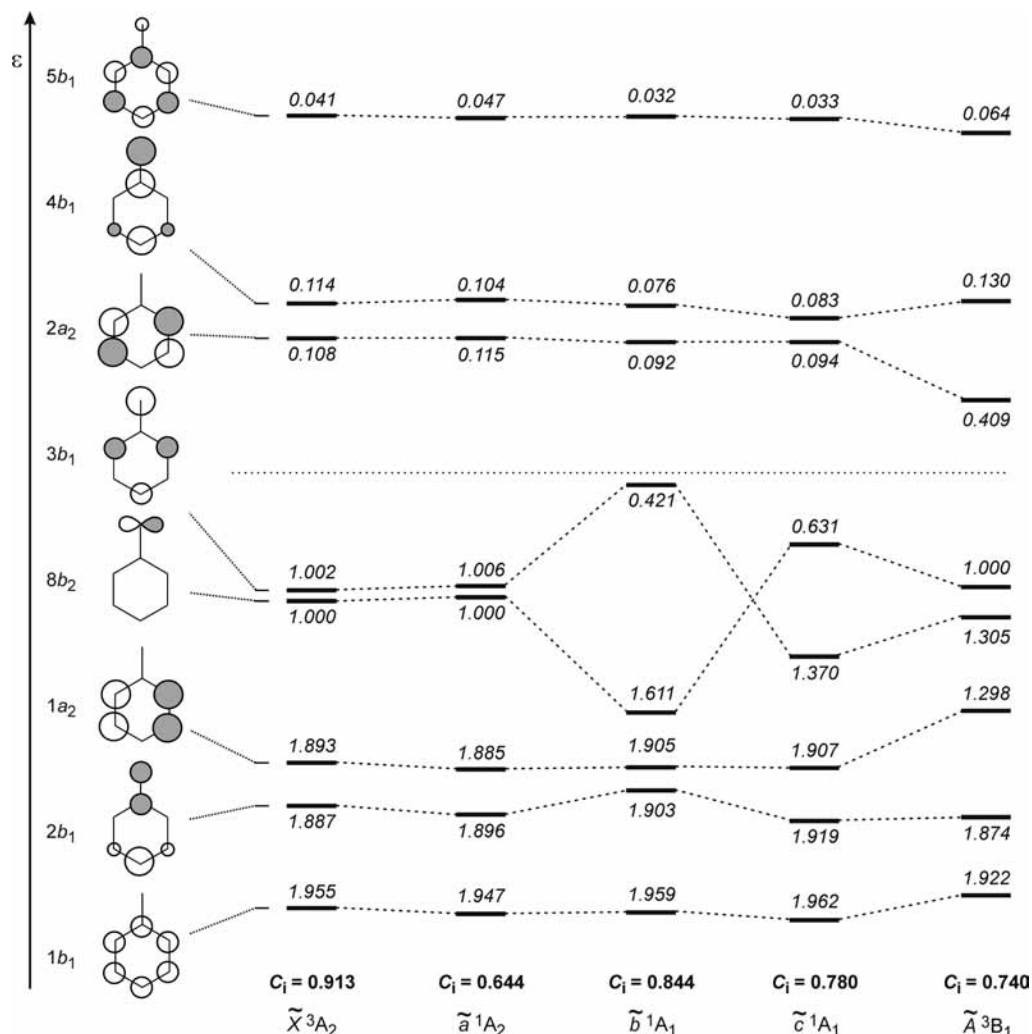


Figure 1. Orbital energy diagram for leading configurations of phenylnitrene (**1**) in the five lowest electronic states. Occupation numbers of natural orbitals are given in italics, and the CI coefficient (C_i) of the respective configuration in the CASSCF wave function is given in bold.

pure spherical harmonics) was used throughout, where the cardinal number X equals 2, 3, and 4 for double- ξ , triple- ξ , and quadruple- ξ basis sets ($X = D, T, Q$), respectively.¹¹ The computed energies were extrapolated to the complete basis set limit (CBL) according to eq 1 (for details, see ref 12).

$$E(X) = E_\infty + AX^{-3} + BX^{-5} \quad (1)$$

Geometry optimizations and frequency calculations were carried out with Gaussian 98,¹³ whereas energies were obtained with the MOLPRO 2000.1 suite of programs.¹⁴

Results and Discussion

Initial calculations of the two or three lowest roots in each irreducible representation were carried out at the CASSCF/cc-pVTZ level, and energies were refined employing the ACPF/cc-pVTZ method. Structures of the three lowest electronic states of **1** and vertical excitation energies to all singlet and triplet states within 100 kcal mol⁻¹ of the ground-state energy (at the CASSCF level) are summarized in Figure 2 and Table 1.

At the ACPF level, the adiabatic ΔE_{ST} of **1** is 17.5 kcal mol⁻¹, in good agreement with previous calculations employing the CAS(2,2)-CISD (17.6 kcal mol⁻¹) or CAS(8,8)-MP2 methods (18.0 kcal mol⁻¹) in combination with the same basis set.^{5b} The similarity of these numbers and the ACPF and CASSCF energies indicates little influence of dynamical electron correlation effects

on the relative energies of these states. Inclusion of zero-point vibrational energy corrections (ZPE) lowers ΔE_{ST} by 0.5 kcal mol⁻¹. However, the calculated splitting is still larger than the revised experimental number by 2.0 kcal mol⁻¹ and actually comes closer to the original value and to early computational results using less flexible basis sets.^{1,3} Given the importance of this value in phenylnitrene chemistry, a closer look seemed to be warranted. To gain quantitative accuracy, the adiabatic and vertical singlet–triplet energy splittings were computed by various multireference methods in combination with increasingly flexible basis sets and extrapolation to the CBL (Table 2).

According to these data, the best estimate for the adiabatic ΔE_{ST} is 15.9 kcal mol⁻¹, in reasonable agreement with the revised experimental value. Obviously, basis set effects play a more important role than the different ways of the N electron treatment for these states of **1**. It is remarkable that RS2 performs even slightly worse than CASSCF as compared to the measured value and MRCI computations, but the overall variations among different methods are extremely small. Interestingly, reduction of the active space to a single configuration produces rather accurate CISD data, but in this case, the Davidson correction turns out to have a profound influence on ΔE_{ST} that is underestimated by 1 kcal mol⁻¹ at the CISD + Q level in the complete basis set limit. The best estimates for the vertical singlet–triplet splittings at the geometry of the ground state

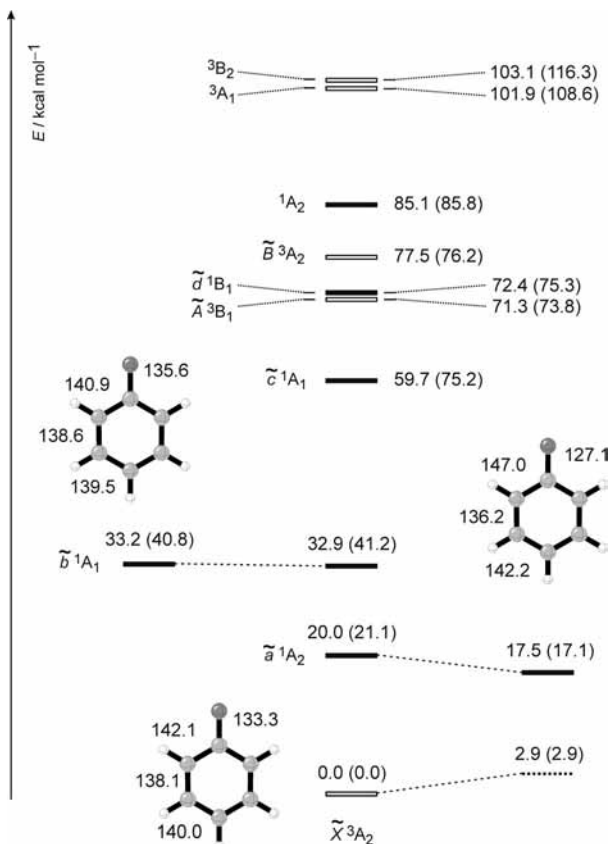


Figure 2. Equilibrium geometries (heavy atom bond lengths in pm) of the three lowest electronic states (CASSCF(8,8)/cc-pVTZ) and energies of various excited states of **1** computed at the ACPF/cc-pVTZ level. CASSCF energies are given in parentheses.

TABLE 1: Vertical CASSCF/cc-pVTZ and ACPF/cc-pVTZ Energies of the Lowest Singlet and Triplet States of **1 (kcal mol⁻¹)^a**

state	E_{CASSCF}	leading configurations	C_i	E_{ACPF}
\tilde{X}^3A_2	0.0	$(1b_1)^2(2b_1)^2(1a_2)^2(8b_2)^1(3b_1)^1$	0.913	0.0
\tilde{a}^1A_2	21.1	$(1b_1)^2(2b_1)^2(1a_2)^2(8b_2)^+(3b_1)^-$ $(1b_1)^2(2b_1)^2(1a_2)^2(8b_2)^-(3b_1)^+$	0.644 0.644	20.0
\tilde{b}^1A_1	41.2	$(1b_1)^2(2b_1)^2(1a_2)^2(8b_2)^2$ $(1b_1)^2(2b_1)^2(1a_2)^2(3b_1)^2$	0.844 0.411	32.9
\tilde{c}^1A_1	75.2	$(1b_1)^2(2b_1)^2(1a_2)^2(3b_1)^2$ $(1b_1)^2(2b_1)^2(1a_2)^2(8b_2)^2$	0.780 0.520	59.7
\tilde{A}^3B_1	73.8	$(1b_1)^2(2b_1)^2(1a_2)^1(3b_1)^2(8b_2)^1$ $(1b_1)^2(2b_1)^2(1a_2)^2(8b_2)^1(2a_2)^1$	0.740 0.501	71.3
\tilde{d}^1B_1	75.3	$(1b_1)^2(2b_1)^2(1a_2)^+(3b_1)^2(8b_2)^-$ $(1b_1)^2(2b_1)^2(1a_2)^-(3b_1)^2(8b_2)^+$ $(1b_1)^2(2b_1)^2(1a_2)^2(8b_2)^+(2a_2)^-$ $(1b_1)^2(2b_1)^2(1a_2)^2(8b_2)^-(2a_2)^+$	0.534 0.534 0.350 0.350	72.4
\tilde{B}^3A_2	76.2	$(1b_1)^2(1a_2)^2(2b_1)^1(3b_1)^2(8b_2)^1$ $(1b_1)^2(1a_2)^2(2b_1)^2(8b_2)^1(4b_1)^1$ $(1b_1)^2(1a_2)^2(2b_1)^2(3b_1)^1(8b_2)^1$ $(1b_1)^2(1a_2)^2(2b_1)^+(3b_1)^-(8b_2)^+(4b_1)^+$	0.597 0.463 0.350 0.294	77.5
1A_2	85.8	8 dets		85.1

^a Leading configurations together with corresponding C_i coefficients are given for comparison.

and at the \tilde{a}^1A_2 geometry are 18.9 and 13.8 kcal mol⁻¹, respectively.

For many closed-shell singlet biradicals, it was found that unrestricted DFT can give qualitatively and often quantitatively correct structures, properties, and energies, even within a single-reference approach.¹⁵ Because DFT has been used extensively to study rearrangements of phenylnitrenes as well as excited

TABLE 2: Adiabatic and Vertical Singlet–Triplet Energy Splittings of **1 (kcal mol⁻¹)^a**

method ^b	cc-pVDZ	cc-pVTZ	cc-pVQZ	CBL
$\tilde{a}^1A_2 \leftarrow \tilde{X}^3A_2$				
SCF ^c	22.8 (22.3)	21.6 (21.1)	21.3 (20.8)	21.1 (20.6)
CISD ^c	19.0 (18.5)	17.6 (17.1)	17.0 (16.5)	16.5 (16.0)
CISD + Q ^c	17.1 (16.6)	15.6 (15.1)	15.0 (14.5)	14.5 (14.0)
SCF	17.8 (17.4)	17.1 (16.6)	16.9 (16.5)	16.7 (16.3)
RS2	19.2 (18.7)	18.0 (17.5)	17.5 (17.0)	17.1 (16.6)
RS3	19.0 (18.5)	17.5 (17.0)	16.9 (16.4)	16.4 (15.9)
CISD	18.4 (18.0)	17.2 (16.7)	16.7 (16.3)	16.3 (15.8)
CISD + Q	18.5 (18.0)	17.1 (16.6)	16.6 (16.1)	16.2 (15.7)
AQCC	18.9 (18.4)	17.5 (17.0)	16.9 (16.4)	16.4 (15.9)
ACPF	18.9 (18.4)	17.5 (17.0)	16.9 (16.4)	16.5 (16.0)
$\tilde{a}^1A_2/\tilde{X}^3A_2 \leftarrow \tilde{X}^3A_2$				
SCF	21.8	21.1	21.0	20.9
RS2	21.4	19.9	19.3	18.7
RS3	22.0	20.2	19.6	19.0
CISD	21.6	20.2	19.7	19.3
CISD + Q	21.5	19.8	19.3	18.8
AQCC	21.73	20.01	19.42	18.9
ACPF	21.74	19.99	19.39	18.9
$\tilde{a}^1A_2 \leftarrow \tilde{X}^3A_2/\tilde{a}^1A_2$				
SCF	14.7	14.2	14.1	14.0
RS2	16.6	15.6	15.2	14.9
RS3	15.6	14.3	13.9	13.5
CISD	15.3	14.2	13.9	13.6
CISD + Q	15.5	14.3	14.0	13.6
AQCC	15.8	14.6	14.2	13.8
ACPF	15.8	14.6	14.2	13.9

^a Values in parentheses include ZPE corrections (CASSCF(8,8)/cc-pVTZ). ^b Energies based on a CASSCF(8,8) wave function and CASSCF(8,8)/cc-pVTZ geometries, if not mentioned otherwise. ^c Energies based on a CASCF(2,2) reference that reduces to a single-configurational description of the ground state and a single-configurational, two-determinantal description of the singlet state.

TABLE 3: Adiabatic Singlet–Triplet Energy Splitting of **1 (kcal mol⁻¹) Calculated at the UDFL Level^a**

method	cc-pVDZ	cc-pVTZ	cc-pVQZ
BVWN	9.5 (9.6)	9.1 (9.2)	8.9
BLYP	9.9 (10.0)	9.3 (9.5)	9.2
BPW91	10.9 (11.0)	10.4 (10.5)	10.3
B3LYP	12.8 (13.1)	12.3 (12.5)	12.2
mPW1LYP	13.3 (13.6)	12.7 (13.0)	12.5
B3PW91	13.8 (14.1)	13.3 (13.6)	13.2
mPW1PW91	14.4 (14.7)	13.9 (14.2)	13.7
BHandHLYP	16.4 (17.0)	15.8 (16.3)	15.7

^a Values in parentheses include ZPE corrections.

states of substituted derivatives of **1**,^{1,3} different functionals were investigated to evaluate the performance of this low-cost approach. From the data shown in Table 3, it is evident that most functionals underestimate ΔE_{ST} by varying amounts. This finding is not surprising, given the substantial spin contamination of the singlet states; in all cases, the $\langle S^2 \rangle$ expectation value is close to unity. The spin contamination of the triplet state that is well-described by a single configuration is negligible for all functionals, with $\langle S^2 \rangle$ expectation values ranging from 2.02 to 2.14. As a consequence, the variability in ΔE_{ST} among different functionals is not reduced when the triplet contamination is projected out (e.g., via common sum formula schemes).

Whereas the equilibrium geometry of the \tilde{a}^1A_2 state of **1** differs considerably from the ground-state structure, the closed-shell singlet \tilde{b}^1A_1 shows similar bond lengths and angles as \tilde{X}^3A_2 .³ Accordingly, vertical and adiabatic excitation energies

TABLE 4: Adiabatic and Vertical Excitation Energies to the \tilde{b}^1A_1 State of **1 (kcal mol⁻¹)**

method ^a	cc-pVDZ	cc-pVTZ	cc-pVQZ	CBL
$\tilde{b}^1A_1 \leftarrow \tilde{X}^3A_2$				
SCF	42.1	40.8	40.5	40.2
RS2	37.2	34.5	33.4	32.4
RS3	36.0	33.0	31.8	30.7
CISD	38.2	35.8	34.9	34.2
CISD + Q	36.7	33.8	32.8	31.9
AQCC	36.6	33.6	32.4	31.4
ACPF	36.4	33.2	32.0	31.0
$\tilde{b}^1A_1/\tilde{X}^3A_2 \leftarrow \tilde{X}^3A_2$				
SCF	42.6	41.3	40.9	40.6
RS2	37.1	34.4	33.2	32.2
RS3	35.7	32.6	31.3	30.1
CISD	38.2	35.8	34.9	34.1
CISD + Q	36.5	33.6	32.5	31.5
AQCC	36.4	33.3	32.1	31.1
ACPF	36.2	32.9	31.7	30.6

^a Energies based on a CASSCF(8,8) wave function and CASSCF-(8,8)/cc-pVTZ geometries.

TABLE 5: Vertical Excitation Energies to the \tilde{c}^1A_1 , \tilde{A}^3B_1 , and \tilde{d}^1B_1 States of **1 (kcal mol⁻¹)**

method ^a	cc-pVDZ	cc-pVTZ	cc-pVQZ	CBL
$\tilde{c}^1A_1/\tilde{X}^3A_2 \leftarrow \tilde{X}^3A_2$				
SCF	76.2	75.2	74.9	74.7
RS2	57.1	54.1	52.8	51.6
CISD	65.0	63.4	62.7	62.1
CISD + Q	58.7	56.9	56.1	55.4
ACPF	62.2	59.7	58.6	57.6
$\tilde{A}^3B_1/\tilde{X}^3A_2 \leftarrow \tilde{X}^3A_2$				
SCF	74.6	73.8	73.6	73.5
CISD	74.1	72.6	72.3	72.0
CISD + Q	73.5	71.9	71.5	71.1
ACPF	73.2	71.4	70.8	70.4
$\tilde{d}^1B_1/\tilde{X}^3A_2 \leftarrow \tilde{X}^3A_2$				
SCF	76.1	75.3	75.1	74.9
CISD	75.4	73.8	73.4	73.1
CISD + Q	74.8	73.0	72.5	72.1
ACPF	74.4	72.4	71.8	71.4

^a Energies based on a CASSCF(8,8) wave function and CASSCF-(8,8)/cc-pVTZ geometries.

to this state are rather identical (Table 4). At the CASCF level, the optimized structure of \tilde{b}^1A_1 is only 0.4 kcal mol⁻¹ lower in energy as compared to the vertical excitation energy (40.6 kcal mol⁻¹). However, employing correlated electronic structure methods, the excitation energy is lowered significantly, and both vertical and adiabatic energies of the \tilde{b}^1A_1 state are 31.0 ± 1 kcal mol⁻¹. The adiabatic excitation energy is even slightly higher than the vertical gap, indicating the necessity to include dynamical correlation effects for a proper description of the closed-shell singlet state.

The energies of the next higher singlet and triplet states are summarized in Table 5. Similar to \tilde{b}^1A_1 , the \tilde{c}^1A_1 state requires inclusion of dynamical correlation to avoid significant overestimation of the excitation energy. In contrast to the former, however, different correlated methods lead to varying excitation energies between 52 (RS2) and 62 (CISD) kcal mol⁻¹. As a best estimate for the \tilde{c}^1A_1 state of **1**, we consider the CISD + Q and ACPF energies of 56–57 kcal mol⁻¹ but note that the uncertainty in this case is slightly larger than for the other excited states of **1** discussed previously. The first excited triplet state \tilde{A}^3B_1 is consistently predicted to be 70–71 kcal mol⁻¹ above the ground state and almost degenerate with the \tilde{d}^1B_1

state of phenylnitrene. According to the best estimate, the latter is 1–2 kcal mol⁻¹ less stable than the triplet.

Conclusion

In summary, the first excited singlet and triplet states of phenylnitrene were investigated using various multireference configuration interaction and perturbation theory methods. The vertical and adiabatic singlet–triplet energy splittings of **1** are 18.9 and 15.9 kcal mol⁻¹, respectively, the latter in good agreement with the revised experimental value of 15.1 ± 0.2 kcal mol⁻¹. The next higher states are \tilde{b}^1A_1 (31 kcal mol⁻¹), \tilde{c}^1A_1 (57 kcal mol⁻¹), \tilde{A}^3B_1 (71 kcal mol⁻¹), and \tilde{d}^1B_1 (72 kcal mol⁻¹). The use of sufficiently flexible basis sets turns out to be crucial to obtain accurate excitation energies of phenylnitrene.

Acknowledgment. I am very thankful to Profs. Wolfram Sander and Frank Würthner for their support and encouragement and for access to computational facilities used in this research. Financial support by the Fonds der Chemischen Industrie through a Liebig fellowship is gratefully acknowledged.

References and Notes

- (1) Selected reviews on arylnitrene chemistry: (a) Schuster, G. B.; Platz, M. S. *Adv. Photochem.* **1992**, *17*, 69. (b) Borden, W. T.; Gritsan, N. P.; Hadad, C. M.; Karney, W. L.; Kemnitz, C. R.; Platz, M. S. *Acc. Chem. Res.* **2000**, *33*, 765. (c) Gritsan, N. P.; Platz, M. S. *Adv. Phys. Org. Chem.* **2001**, *36*, 255. (d) Platz, M. S. In *Reactive Intermediate Chemistry*; Moss, R. A.; Platz, M. S., Jones, M., Jr., Eds.; Wiley: New York, 2004. (e) Gritsan, N. P.; Platz, M. S. *Chem. Rev.* **2006**, *106*, 3844.
- (2) (a) Smolinsky, G.; Wasserman, E.; Yager, W. A. *J. Am. Chem. Soc.* **1962**, *84*, 3220. (b) Travers, M. J.; Cowles, D. C.; Clifford, E. P.; Ellison, G. B. *J. Am. Chem. Soc.* **1992**, *114*, 8699. (c) McDonald, R. N.; Davidson, S. J. *J. Am. Chem. Soc.* **1993**, *115*, 10857. (d) Gritsan, N. P.; Yuzawa, T.; Platz, M. S. *J. Am. Chem. Soc.* **1997**, *119*, 5059. (e) Warmuth, R.; Makowiec, S. *J. Am. Chem. Soc.* **2007**, *129*, 1233.
- (3) (a) Kim, S. J.; Hamilton, T. P.; Schaefer, H. F., III *J. Am. Chem. Soc.* **1992**, *114*, 5349. (b) Hrovat, D. A.; Waali, E. E.; Borden, W. T. *J. Am. Chem. Soc.* **1992**, *114*, 8698. (c) Smith, B. A.; Cramer, C. J. *J. Am. Chem. Soc.* **1996**, *118*, 5490. (d) Castell, O.; Garcia, V. M.; Bo, C.; Caballero, R. *J. Comput. Chem.* **1996**, *17*, 42. (e) Karney, W. L.; Borden, W. T. *J. Am. Chem. Soc.* **1997**, *119*, 1378. (f) Kemnitz, C. R.; Karney, W. L.; Borden, W. T. *J. Am. Chem. Soc.* **1998**, *120*, 3499. (g) Gritsan, N. P.; Zhu, Z.; Hadad, C. M.; Platz, M. S. *J. Am. Chem. Soc.* **1999**, *121*, 1202. (h) Johnson, W. T. G.; Sullivan, M. B.; Cramer, C. J. *Int. J. Quantum Chem.* **2001**, *85*, 492. (i) Karney, W. L.; Borden, W. T. In *Advances in Carbene Chemistry*; Brinker, U. H., Ed.; Elsevier: Amsterdam, 2001; Vol. 3, p 205. (j) Tsao, M.-L.; Platz, M. S. *J. Am. Chem. Soc.* **2003**, *125*, 12014.
- (4) (a) Wenthold, P. G., personal communication. (b) Wijerathne, N.; Wenthold, P. G. *4th Heron Island Conference on Reactive Intermediates and Unusual Molecules (Heron 4)*, Heron Island, Great Barrier Reef, Queensland, Australia, July 7–14, 2007.
- (5) (a) Wenk, H.-H.; Sander, W. *Angew. Chem.* **2002**, *114*, 2873; *Angew. Chem., Int. Ed.* **2002**, *41*, 2742. (b) Bettinger, H. F.; Sander, W. *J. Am. Chem. Soc.* **2003**, *125*, 9726. (c) Sander, W.; Winkler, M.; Cakir, B.; Grote, D.; Bettinger, H. F. *J. Org. Chem.* **2007**, *72*, 715. (d) Sander, W.; Grote, D.; Kossmann, S.; Neese, F. *J. Am. Chem. Soc.* **2008**, *130*, 4396.
- (6) (a) Werner, H.-J.; Knowles, P. J. *J. Chem. Phys.* **1985**, *82*, 5053. (b) Knowles, P. J.; Werner, H.-J. *Chem. Phys. Lett.* **1985**, *115*, 259.
- (7) Werner, H.-J. *Mol. Phys.* **1996**, *89*, 645.
- (8) (a) Werner, H.-J. *Adv. Chem. Phys.* **1987**, *59*, 1. (b) Werner, H.-J.; Knowles, P. J. *J. Chem. Phys.* **1988**, *89*, 5803. (c) Knowles, P. J.; Werner, H.-J. *Chem. Phys. Lett.* **1988**, *145*, 514.
- (9) (a) Langhoff, S. R.; Davidson, E. R. *Int. J. Quantum Chem.* **1974**, *8*, 61. (b) Duch, W.; Dierksen, G. H. F. *J. Chem. Phys.* **1994**, *101*, 3018.
- (10) (a) Gdanitz, R. J.; Ahlrichs, R. *Chem. Phys. Lett.* **1988**, *143*, 413. (b) Szalay, P. G.; Bartlett, R. J. *J. Phys. Chem.* **1995**, *103*, 3600.
- (11) (a) Dunning, T. H. *J. Chem. Phys.* **1989**, *90*, 1007. (b) Kendall, R. A.; Dunning, T. H.; Harrison, R. J. *J. Chem. Phys.* **1992**, *96*, 6796. (c) Woon, D. E.; Dunning, T. H. *J. Chem. Phys.* **1993**, *98*, 1358. (d) Woon, D. E.; Dunning, T. H., Jr. *J. Chem. Phys.* **1994**, *100*, 2975.
- (12) (a) Kutzelnigg, W.; Morgan, J. D. *J. Chem. Phys.* **1992**, *96*, 4484. See also: (b) Lindh, R.; Bernhardsson, A.; Schütz, M. *J. Phys. Chem. A* **1999**, *103*, 9913, and references therein. (c) Dunning, J. H., Jr. *J. Phys. Chem. A* **2000**, *104*, 9062. (d) Dunning, J. H., Jr.; Peterson, K. A. *J. Chem. Phys.* **2000**, *113*, 7799. (e) Petersson, G. A.; Frisch, M. J. *J. Phys. Chem. A* **2000**, *104*, 2183.

(13) Frisch, M. J.; Trucks, G. W.; Schlegel, H. B.; Scuseria, G. E.; Robb, M. A.; Cheeseman, J. R.; Zakrzewski, V. G.; Montgomery, J. A., Jr.; Stratmann, R. E.; Burant, J. C.; Dapprich, S.; Millam, J. M.; Daniels, A. D.; Kudin, K. N.; Strain, M. C.; Farkas, O.; Tomasi, J.; Barone, V.; Cossi, M.; Cammi, R.; Mennucci, B.; Pomelli, C.; Adamo, C.; Clifford, S.; Ochterski, J.; Petersson, G. A.; Ayala, P. Y.; Cui, Q.; Morokuma, K.; Malick, D. K.; Rabuck, A. D.; Raghavachari, K.; Foresman, J. B.; Cioslowski, J.; Ortiz, J. V.; Stefanov, B. B.; Liu, G.; Liashenko, A.; Piskorz, P.; Komaromi, I.; Gomperts, R.; Martin, R. L.; Fox, D. J.; Keith, T.; Al-Laham, M. A.; Peng, C. Y.; Nanayakkara, A.; Gonzalez, C.; Challacombe, M.; Gill, P. M. W.; Johnson, B.; Chen, W.; Wong, M. W.; Andres, J. L.; Gonzalez, C.; Head-Gordon, M.; Replogle, E. S.; Pople, J. A. *Gaussian 98*; Gaussian, Inc.: Pittsburgh, PA, 1998.

(14) Werner, H.-J.; Knowles, P. J. *Molpro 2000.1*; Birmingham, 1999.

(15) Koch, W.; Holthausen, M. C. *A Chemist's Guide to Density Functional Theory*; Wiley-VCH: Weinheim, Germany, 2000. and references therein. (a) See also: (b) Gräfenstein, J.; Hjerpe, A. M.; Kraka, E.; Cremer, D. *J. Phys. Chem. A* **2000**, *104*, 1748. (c) Polo, V.; Kraka, E.; Cremer, D. *Theor. Chem. Acc.* **2002**, *107*, 291. (d) Polo, V.; Kraka, E.; Cremer, D. *Mol. Phys.* **2002**, *100*, 1771. (e) Winkler, M. *J. Phys. Chem. A* **2005**, *109*, 1240.

JP802547C